

# On Statistical Lensing and the Anti-Correlation Between 2dF QSOs and Foreground Galaxies

A. D. Myers<sup>1,6\*</sup>, P. J. Outram<sup>1</sup>, T. Shanks<sup>1</sup>, B. J. Boyle<sup>2</sup>, S. M. Croom<sup>2</sup>,  
N. S. Loaring<sup>3</sup>, L. Miller<sup>4</sup>, & R. J. Smith<sup>5</sup>

<sup>1</sup> Department of Physics, Science Laboratories, South Road, Durham, DH1 3LE, U.K.

<sup>2</sup> Anglo-Australian Observatory, PO Box 296, Epping, NSW 2121, Australia

<sup>3</sup> Mullard Space Science Laboratory, University College London, Holmbury St. Mary, Dorking, Surrey, RH5 6NT, U.K.

<sup>4</sup> Department of Physics, Oxford University, Keble Road, Oxford, OX1 3RH, U.K.

<sup>5</sup> Liverpool John Moores University, Twelve Quays House, Egerton Wharf, Birkenhead, CH41 1LD, U.K.

<sup>6</sup> Department of Astronomy, University of Illinois, 1002 W Green Street, Urbana, IL 61801, U.S.A.

25 July 2021

## ABSTRACT

We study the cross-correlation of APM and SDSS galaxies with background QSOs taken from the 2dF QSO Redshift Survey, and detect a significant ( $2.8\sigma$ ) anti-correlation. The lack of a similar signal between stars in the 2dF survey and our galaxy samples gives us confidence that the anti-correlation is not due to a systematic error. The possibility that dust in the foreground galaxies could produce such an anti-correlation is marginally rejected, at the  $2\sigma$  level through consideration of the colours of QSOs behind these galaxies. It is possible that a dust model that obscures QSOs without reddening them, or preferentially discards reddened QSOs from the 2QZ sample, could produce such an anti-correlation, however, such models are at odds with the positive QSO-galaxy correlations found at bright magnitudes by other authors.

Our detection of a galaxy-QSO anti-correlation is consistent with the predictions of statistical lensing theory. When combined with earlier results that have reported a *positive* galaxy-QSO correlation, a consistent and compelling picture emerges that spans faint and bright QSO samples showing positive or negative correlations according to the QSO  $N(m)$  slope.

We find that galaxies are highly anti-biased on small scales. We consider two models that use quite different descriptions of the lensing matter and find they yield consistent predictions for the strength of galaxy bias on  $0.1 h^{-1}\text{Mpc}$  scales of  $b \sim 0.1$  (for a  $\Lambda\text{CDM}$  cosmology). Whilst the slope of our power-law fit to the QSO-galaxy cross-correlation does not allow us to rule out a linear bias parameter, when we compare our measurement of  $b$  on  $100 h^{-1}\text{kpc}$  scales to independent methods that determine  $b \sim 1$  on  $h^{-1}\text{Mpc}$  scales, we conclude that bias, on these small scales, is scale-dependent. These results indicate that there appears to be more mass present, at least on the  $100 h^{-1}\text{kpc}$  scales probed, than predicted by simple  $\Lambda\text{CDM}$  biasing prescriptions, and thus constrains halo occupation models of the galaxy distribution.

**Key words:** surveys - quasars, quasars: general, large-scale structure of Universe, cosmology: observations, gravitational lensing

## 1 INTRODUCTION

Intervening massive structures can, via weak gravitational lensing, alter the density of high-redshift objects detected

behind them. Myers et al. (2003) demonstrated the anti-correlation between faint QSOs and groups of galaxies, confirming the earlier detection by Boyle, Fong & Shanks (1988). Using models of lensing by simple haloes (Croom & Shanks 1999) they concluded that, if due to gravitational lensing, the observed anti-correlation favoured more mass

\* E-mail: adm@astro.uiuc.edu

in groups of galaxies than accounted for in a universe with density parameter  $\Omega_m = 0.3$ .

Though statistical lensing is most apparent for larger concentrations of mass, such as groups of galaxies, most recent attempts to measure and model associations between QSOs and foreground mass have focussed on the cross-correlation between QSOs and individual galaxies. Seldner & Peebles (1979) were among the first authors to record a statistically significant clustering of individual galaxies with bright, high-redshift QSOs, although Tyson (1986) appears to be the first to have mentioned lensing as a possible explanation. Webster et al. (1988) developed a statistical lensing explanation for the association of QSOs with foreground galaxies, suggesting that more lensing mass must be being traced than expected (Kovner 1989; Narayan 1989; Schneider 1989). Since then, more authors have found positive correlations between optically-selected QSOs and galaxies (Thomas, Webster & Drinkwater 1995; Williams & Irwin 1998). Many more have measured positive correlations between galaxies and radio-selected QSOs (Fugmann 1990; Bartsch, Schneider & Bartelmann 1997; Benitez & Martinez-Gonzalez 1997; Norman & Williams 2000), for which a larger lensing effect is expected. Very few *anti*-correlations between QSOs and galaxies have been detected (Benitez & Martinez-Gonzalez 1997; Ferreras et al. 1997), and these were mainly attributed to QSO-selection effects. However, as detected by Myers et al. (2003), an anti-correlation between *faint* QSOs and foreground matter is predicted by statistical lensing.

The galaxy distribution, relative to underlying mass, is a function of bias, whereas the QSO distribution directly traces the mass that lensed it. Thus, comparing the QSO-galaxy cross-correlation to the galaxy auto-correlation can be used to constrain galaxy bias. Recent observations of positive correlations between bright QSOs and galaxies (Williams & Irwin 1998; Gaztañaga 2003) suggest a very low value for the bias parameter ( $b \sim 0.1$ ). The work of Gaztañaga (2003) suggests  $b \sim 0.1$  on sub-Megaparsec scales. The work of Williams & Irwin (1998) suggests  $b \sim 0.1$  on Megaparsec scales but is consistent with  $b \sim 0.1$  on sub-Megaparsec scales. However, measurements of the strength of bias from clustering in galaxy surveys out to (redshift)  $z \sim 0.2$  (Verde et al. 2002), comparisons of local galaxy clustering with the Cosmic Microwave Background (Lahav et al. 2002) and weak lensing shear (Hoekstra et al. 2002) at  $z \sim 0.35$ , seem to converge on a linear model of bias with  $b$ , of the order of unity on scales of 5 – 100 Mpc. Taken together, these results suggest that either there is a strong scale-dependence to bias, or that there exists an unexpected, strong systematic effect inducing positive correlations between QSOs and foreground galaxies.

The faint flux limit of the 2dF QSO Redshift Survey (Croom et al. 2004), henceforth referred to as the ‘2QZ’, may test these two possibilities. As the 2QZ number-magnitude count slope at the survey flux limit is relatively flat, statistical lensing predicts an anti-correlation between 2QZ QSOs and foreground galaxies, as opposed to the positive correlations predicted for brighter QSO samples and detected by Williams & Irwin (1998) and Gaztañaga (2003). As there is no other explanation for such opposite signals in the different samples, such a detection would provide a strong confirmation of the lensing hypothesis, and hence the constraints on  $b$ . There are additional reasons why the 2QZ is appropriate

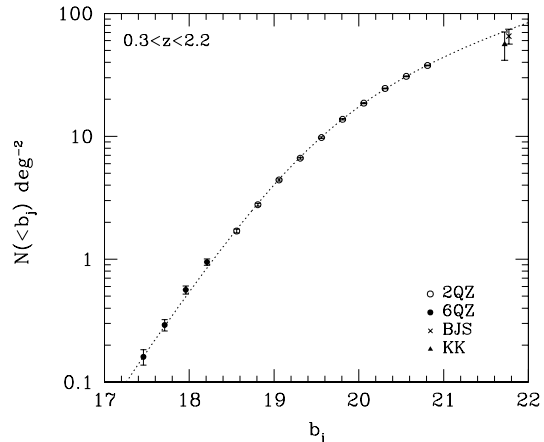


**Figure 1.** The QSO integrated number counts, for the 2QZ, in 0.2 mag bins, with Poisson errors. The line is a smoothed power law fit to the differential number counts. Brighter data points are from the 6QZ. Also displayed are the faint data from Boyle, Jones & Shanks (1991) and Koo & Kron (1988), which have been offset slightly to prevent the points from merging.

to study statistical lensing. The 2QZ contains around half as many confirmed stars as QSOs, which may be used as a control, to determine if any cross-correlation arises from target-selection. The 2QZ can limit the most likely systematic, intervening dust—by considering QSO colours, the extent that dust in galaxies could obscure background QSOs may be determined. Finally, the known redshifts of 2QZ QSOs can ensure that they are physically removed from a galaxy sample.

This paper regards the cross-correlation between faint QSOs and foreground galaxies, and its implications for cosmological parameters, particularly for galaxy bias. In Section 2 we outline the samples of QSOs and galaxies we shall cross-correlate. In Section 3 we outline our cross-correlation methodology, and investigate possible explanations for the resulting signal. Section 4 introduces models we use to investigate the cross-correlation of QSOs and galaxies in terms of statistical lensing. Section 5 applies these lensing models and discusses implications for cosmological parameters, especially how galaxies are biased relative to underlying matter. Finally, in Section 6, we summarise the main results of this paper.

## 2 QSO AND GALAXY SAMPLES

The QSO and galaxy samples we will cross-correlate are essentially the same as described by Myers et al. (2003), so we will only outline them briefly. QSOs are taken from the final 2QZ catalogue (Croom et al. 2004). The 2QZ comprises two 5 deg  $\times$  75 deg declination strips, one in an equatorial region in the North Galactic Cap (centred at  $\delta = 0^\circ$  with  $09^{\text{h}}50^{\text{m}} \lesssim \alpha \lesssim 14^{\text{h}}50^{\text{m}}$ ), and one at the South Galactic Pole (centred at  $\delta = -30^\circ$ , with  $21^{\text{h}}40^{\text{m}} \lesssim \alpha \lesssim 03^{\text{h}}15^{\text{m}}$ ). We will refer to these regions as the ‘NGC’ and ‘SGC’ respectively. QSOs are selected by ultra-violet excess (UVX) in the  $u - b_J : b_J - r$  plane, in the magnitude range  $18.25 \leq b_J \leq 20.85$ . The 2QZ

colour selection is  $\gtrsim 90$  per cent complete for UVX QSOs over the redshift range  $0.3 < z < 2.2$ . At higher redshifts the UVX technique fails as the Lyman-alpha forest enters the  $U$  band, and the completeness of the survey rapidly drops. Unless otherwise specified, we will consider only QSOs with a redshift  $z > 0.4$ , to prevent the overlap in real space of QSO and galaxy samples. We shall work with only the most definitively identified QSO sample, the so-called quality ‘11’ sample. Quality ‘11’ denotes a sample with the best level of reliability for both the QSO identification and redshift estimate (see Croom et al. 2004 for further explanation). These restrictions in redshift and spectroscopic quality leave 12042 QSOs in the SGC and 9565 in the NGC. We shall also consider the supplemental 6dF QSO survey (henceforth 6QZ), which contains 376 QSOs after the application of our  $z > 0.4$  and ‘11’ only spectroscopic identification criteria. For further details of the 2QZ and 6QZ, see Croom et al. (2004).

The expected strength of lensing-induced correlations between galaxies and a magnitude-limited sample of QSOs depends on the slope of the integrated number-magnitude counts,  $\alpha$ , fainter than the QSO sample’s limit (Narayan 1989). An enhancement of QSOs is expected behind foreground lenses when the slope of the QSO number-magnitude counts is greater than 0.4 and a deficit when the slope is less than 0.4. We thus need to estimate this slope for any lensing analysis. In Fig. 1 we reproduce the QSO  $N(< m)$  for the 2QZ from Myers et al. (2003). The points are QSO number counts in 0.2 mag bins with Poisson errors, and have been corrected for incompleteness and absorption by dust in our Galaxy. The line is a smoothed power law fit to the differential counts of form

$$\frac{dN}{dm} = \frac{N_0}{10^{-\alpha_d(m-m_0)} + 10^{-\beta_d(m-m_0)}} \quad (1)$$

with a steep bright-end slope ( $\beta_d = 0.98$ ), a knee at  $m_0 = 19.1$ , and a flatter faint end slope ( $\alpha_d = 0.15$ ). Myers et al. (2003) marginalised across all of the parameters in this fit and determined a faint end slope of  $\alpha = 0.29 \pm 0.015$ , noting that incompleteness corrections might raise the  $1\sigma$  error to as much as 0.05. In this paper, we will assume a slope of  $\alpha = 0.29 \pm 0.03$  at the survey flux limit. Brighter data points are from the 6QZ. Also displayed are the faint data from Boyle, Jones & Shanks (1991) and Koo & Kron (1988), which have been offset slightly to prevent points from merging. Recent observations, attributed to statistical lensing, of positive correlations between QSOs and galaxies (Williams & Irwin 1998; Gaztañaga 2003) have used relatively bright QSO samples, which only probe the steep QSO number-magnitude counts below the knee. The large size and faint flux limit of the 2QZ allows us to probe significantly beyond the knee and test the lensing prediction of an anti-correlation between *faint* QSOs and galaxies.

The southern galaxy sample we consider in this paper is taken from the APM Survey (Maddox et al. 1990b), which is considered photometrically complete to a magnitude of  $b_J < 20.5$  (Maddox et al. 1990a). The northern galaxy sample is taken from the Sloan Digital Sky Survey (henceforth SDSS) Early Data Release (henceforth EDR) of June 2001 (Stoughton et al. 2002). The SDSS EDR sample is transformed into the  $b_J$  band from the SDSS  $g'$  and  $r'$  bands using the colour equations of Yasuda et al. (2001) and cut

to  $b_J < 20.5$  to match the APM limit. Both galaxy samples are restricted to areas in which they overlap the 2QZ strips. This leaves nearly 200,000 galaxies in the SGC 2QZ strip and 100,000 in the NGC 2QZ strip. Note that the SDSS EDR only partially fills the 2QZ NGC strip.

### 3 QSO AND GALAXY CROSS-CORRELATION FUNCTIONS

Correlation functions (Peebles 1980) are the main statistic of choice in studies of how QSO and galaxy distributions are related, although how the statistic is estimated varies considerably. In this section, we measure the two-point cross-correlation between SDSS or APM galaxies and 2QZ (or 6QZ) QSOs. We study possible selection effects and different explanations for the signal. Notably, the expected variation of the QSO-galaxy cross-correlation with redshift and (especially) magnitude of the QSO sample is a strong prediction of the statistical lensing hypothesis, and is something we may be able to test using 2QZ data.

#### 3.1 Correlation Estimator and Errors

To measure the two-point correlation function,  $\omega(\theta)$ , we use the estimator (Peebles 1980)

$$\omega(\theta) = \frac{DD_{12}(\theta)\bar{n}}{DR_{12}(\theta)} - 1, \quad (2)$$

where  $DD_{12}$  denotes the number of data-point *pairs* drawn from populations 1 and 2 respectively with separation  $\theta$ . For  $DR_{12}$  the population 2 data are replaced with a catalogue of random points with the same angular selection function as the data. The factor  $\bar{n}$  is the ratio of the size of the random catalogue to the data. Throughout this paper, we produce random catalogues with  $\bar{n} = 10$ , minimizing statistical noise but allowing efficient speed of calculation. For further details on the 2QZ angular selection function see Outram et al. (2003) and Croom et al. (2004). Note that the cross-correlation function is equivalent in either ‘direction’ (i.e. under the exchange of labels 1 and 2 in Equation 2) *provided that the angular selection of sources is accounted for by an appropriate random catalogue*. In general, the angular selection functions of, say, a galaxy population and a QSO population are not the same. Further, the angular completeness of a given survey is generally a function of redshift and magnitude, so considerable care should be taken in constructing random catalogues for population subsamples.

Numerous estimates of error on the cross-correlation have been proposed. We will consider three of these. One of the simpler forms, is the Poisson error based on the number of data-data pairs (across the entire survey) in the angular bin probed:

$$\sigma_\omega^2(\theta) = \frac{[1 + \omega(\theta)]^2}{DD(\theta)} \quad (3)$$

where we will use  $\sigma_\omega$  to denote the standard error on the correlation function. Given that we wish to measure the significance of the correlation function compared to the null hypothesis represented by the random catalogue, we might instead use the Poisson error based on the number of

data-random pairs, which could be achieved by substituting  $DR/\bar{n}$  for  $DD$  in Equation 3.

The hypothesis that error on the correlation function is Poisson is not strictly fair. All else being equal, the number of counts could be highly correlated as the same points appear in different pairs that are included in many different bins, especially on large scales. Some authors (Shanks & Boyle 1994; Croom & Shanks 1996) have suggested corrections to the Poisson form of error. Instead of such corrections, we will consider errors from field-to-field variations in the correlation function (see, e.g., Stevenson et al. 1985). Our data samples are split into 30 subsamples. This is arbitrary in the case of the SDSS EDR but deliberately reflects plate boundaries in the case of the APM data (and by extension the 2QZ, which is derived from APM photometry). The cross-correlation function is measured for each subsample and the variance between the subsamples is determined. The standard error on  $\omega(\theta)$  is then the standard error between the subsamples, inverse weighted by variance to account for different numbers of objects in each subsample

$$\sigma_{\omega}^2(\theta) = \frac{1}{N-1} \sum_{L=1}^N \frac{DR_L(\theta)}{DR(\theta)} [\omega_L(\theta) - \omega(\theta)]^2. \quad (4)$$

The weighting by number of objects is essential, mainly as plates in the southern APM immediately East of 00h RA cover less area than other plates at the same declination but also because of varying completeness in the QSO catalogue. We will refer to this error as *field-to-field error*.

We will also consider a similar estimate of error to Equation 4, essentially a weighted form of the estimate proposed by Scranton et al. (2002) when calculating the auto-correlation of galaxies in the SDSS EDR

$$\sigma_{\omega}^2(\theta) = \sum_{L'=1}^N \frac{DR_{L'}(\theta)}{DR(\theta)} [\omega_{L'}(\theta) - \omega(\theta)]^2 \quad (5)$$

Note that  $L$  (in Equation 4) refers to a subsample on one of our 30 plates, whereas  $L'$  refers to the subsample remaining *on the other 29 plates*. In other words, the procedure outlined in Equation 5 is to remove each of the plates in turn and to calculate the variance between each sample on the 29 remaining plates. We shall refer to this as *jackknife error*. The unweighted version of this estimate agrees well with simulations (see the appendix of Zehavi et al. 2002).

Finally, we will measure the statistical correlation (not to be confused with the correlation *function*) between adjacent bins of  $w(\theta)$ . The statistical correlation is related to the covariance, and is essentially an estimate of how independent the bins are - whether bin  $i$  has a tendency to take the same value as bin  $j$ . We might expect the covariance of the correlation function to be high, as the same data points can appear in different pairs that are counted in many different bins. The statistical correlation takes the following form

$$Corr(i, j) = \frac{Cov(i, j)}{\sigma(\theta_i)\sigma(\theta_j)} \quad (6)$$

where the covariance,  $Cov(i, j)$ , is defined as

$$Cov(i, j) = \frac{1}{N} \sum_{M=1}^N (\omega_M(\theta_i) - \bar{\omega}(\theta_i))(\omega_M(\theta_j) - \bar{\omega}(\theta_j)) \quad (7)$$

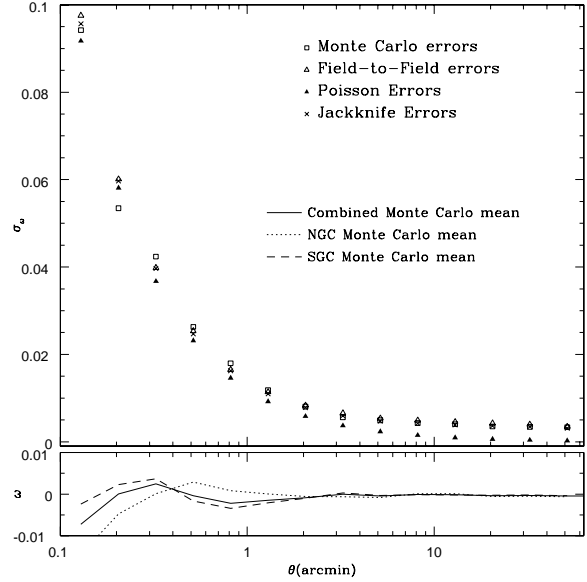


**Figure 2.** In the upper panel, we compare the Poisson, field-to-field and jackknife error estimates with a Monte Carlo error estimate determined from 100 Monte Carlo simulations of the NGC and SGC strips. In the lower panel we plot the mean of the 100 simulations for the NGC and SGC individually and for the NGC and SGC combined.

and  $\theta_i$  and  $\theta_j$  are two bins at different scales, and  $\bar{\omega}$  and  $\sigma$  represent the mean and standard deviation over a number of realisations,  $M$ . The correlation is 0 if the bins are independent, approaches 1 if an increase in bin  $i$  leads to an increase in bin  $j$  and approaches  $-1$  if an increase in bin  $i$  leads to a decrease in bin  $j$ .

To test the accuracy of our correlation function estimator and the associated error, we have created 100 Monte Carlo simulations of the 2QZ. Each simulation contains the same number of ( $z > 0.4$ , identification quality of ‘11’) QSOs as the 2QZ and has the same angular selection function, neglecting any intrinsic QSO clustering. We cross-correlate the simulated samples against APM galaxies (for the SGC strip) and the SDSS EDR (for the NGC strip). For each sample, the estimates of error outlined in this section are calculated and averaged. The mean value of the cross-correlation across the 100 samples is taken and the standard deviation ( $1\sigma$ ) is recorded as the Monte Carlo error. To avoid confusion between our ‘Monte Carlo error’ and the statistical ‘standard error’ we shall refer to the Monte Carlo error as the ‘Monte Carlo deviation’.

In the lower panel of Fig. 2, we display the mean cross-correlation signal across the 100 Monte Carlo simulations. The agreement between the NGC and SGC results are excellent - better than 12 per cent of the Monte Carlo deviation on the NGC mean over all scales. The deviation of the combined result from zero, the expected result, is similarly no more than 12 per cent of the combined Monte Carlo deviation over all scales. We note that the shot noise (i.e. the standard error) would comprise 10 per cent of the Monte Carlo deviation (as we have 100 samples). Although the correlation function diverges on scales smaller than 0.3 arcmin, the error is sufficiently large on these scales that we may

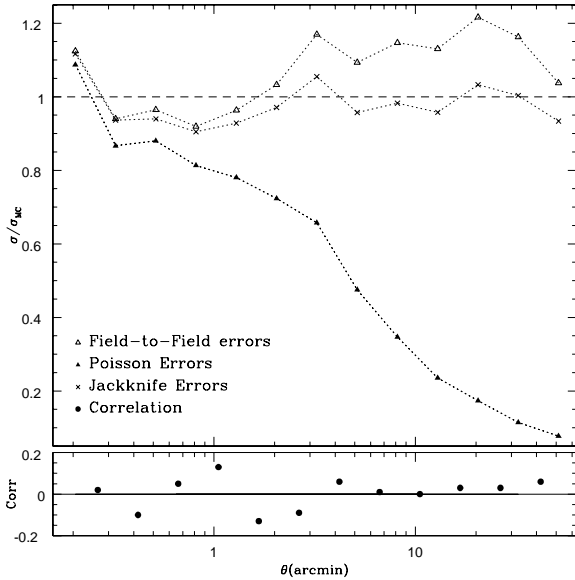


**Figure 3.** In the upper panel we display the error on the correlation function taken in ratio to the Monte Carlo error estimate (1 standard deviation across the Monte Carlo simulations), for each estimate of error mentioned in the text. In all cases the errors are determined for the combined NGC and SGC sample. A dashed line is drawn for comparison at  $\sigma/\sigma_{MC} = 1$  (where the Monte Carlo estimate itself would lie). The lower panel depicts the covariance between adjacent bins determined from 100 Monte Carlo realisations.

consider the correlation estimator probably valid on all of the scales plotted and certainly valid on scales larger than 0.3 arcmin. Note that the consistency of the correlation estimator across all scales indicates that the software we use to calculate the estimator is robust. Also, note that the average Monte Carlo sampling of  $\omega$  contains 1180 random points in the smallest bin and has a jackknife error of 0.098—this means that the typical fluctuation in our random catalog is three-and-a-half times smaller than our quoted error, and is dwarfed by the jackknife error, justifying our choice of  $\bar{n} = 10$  in Equation 2.

In the upper panel of Fig. 2 we compare the various error estimates. The general trend of the errors is in good agreement, although the Poisson error estimate begins to under-predict the error (as compared to the Monte Carlo estimate) on larger scales. We assume that the Monte Carlo deviation represents a fair estimate of the true error on the correlation function and, In Fig. 3, plot the various errors taken in ratio to the Monte Carlo deviation. It is obvious that the Poisson error is an underestimate on  $\gtrsim 5$  arcmin scales. We have also estimated the Poisson error by substituting  $DR$  for  $DD$  in Equation 3. Such a change has negligible effect, as the simulated QSOs have a largely random distribution. The jackknife and field-to-field error estimates are much better than the Poisson estimate and constitute reasonable estimates on scales from 0.2 arcmin to nearly a degree. The field-to-field error, however, is perhaps a 20 per cent overestimate on larger scales, where the jackknife error remains in line with the Monte Carlo estimate. The jackknife error estimate has an additional advantage over the field-to-field estimate. When the number of data

points on any plate approaches zero, the field-to-field estimate is ill-defined but the jackknife estimate remains accurate until the number of data points across the entire survey approaches zero.

In Fig. 3, we also plot the correlation due to the covariance between *adjacent* bins. This covariance is low - almost within the 10 per cent expected standard error. However, this covariance measure demonstrates that no correlation between adjacent bins is artificially introduced by our random catalogues - it does not guarantee that the data will show no covariance. We will quote the significance of results by estimating the correlation function and its associated error in one ‘large’ bin (usually out to 10 arcmin), to minimise any covariance in the data on these scales. Throughout this paper, we adopt the estimate of the correlation function defined by Equation 2, together with the jackknife error estimate of Equation 5 as both seem fair over scales we will probe.

### 3.2 The Cross-Correlation of 2QZ QSOs and Galaxies

In Fig. 4 we plot the cross-correlation of all 2QZ QSOs that meet our selection criteria ( $z > 0.4$  and 2QZ identification of ‘11’) against SDSS EDR galaxies (in the 2QZ NGC strip) and APM galaxies (in the 2QZ SGC strip). The upper panel of Fig. 4 shows the cross-correlation individually for the strips—galaxies are anti-correlated with QSOs in both. The anti-correlation is slightly stronger in the NGC strip but not significantly so. In the lower panel of Fig. 4, we plot the cross-correlation for both ‘directions’. A significant anti-correlation is detected irrespective of whether we centre on galaxies and count QSOs or centre on QSOs and count galaxies, indicating that our random catalogues consistently account for the angular selection of QSOs or galaxies.

If we bin the data displayed in Fig. 4 in a single bin of extent 10 arcmin and estimate the correlation function and ( $1\sigma$ ) jackknife error, we find there is an anti-correlation of strength  $\omega(< 10 \text{ arcmin}) = -0.007 \pm 0.0025$  (10 arcmin is about  $1 h^{-1}\text{Mpc}$  at the median galaxy redshift of 0.15). The significance of this result is  $2.8\sigma$  for  $\omega_{qg}$  and  $2.2\sigma$  for  $\omega_{gq}$ . Although the anti-correlation is slightly less significant for  $\omega_{gq}$ , it is also slightly stronger, i.e.  $\omega(< 10 \text{ arcmin}) = -0.008 \pm 0.0035$ . Further, particularly on large scales ( $> 8\text{arcmin}$ ), the error in  $\omega_{gq}$  is 60-80 per cent of the error in  $\omega_{qg}$ . It is unclear exactly why the errors are slightly larger when the analysis is carried out centring on galaxies but it is likely due to small discrepancies, perhaps second-order gradients, between the random catalogues used to mimic the different angular selection functions of the QSO and galaxy samples.

The anti-correlation displayed in Fig. 4 is very strong on small scales and agreement between the two ‘directions’ of the correlation function is excellent. For instance, both  $\omega_{gq}$  and  $\omega_{qg}$  show an anti-correlation of strength -0.02 out to 3 arcmin at  $3\sigma$  significance. Note that the innermost bin barely contributes to this particular signal, as it contains less than 100th of the pairs in the bin at 2 arcmin. When modelling, we will consider  $\omega_{qg}$ , the slightly weaker, slightly more significant result. This is mainly because ultimately, when discussing the anti-correlation in terms of lensing, we will compare the galaxy-galaxy auto-correlation,

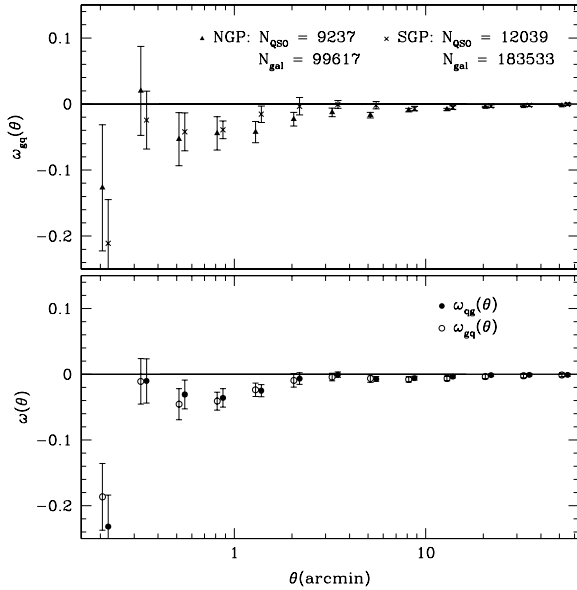


**Figure 4.** The cross-correlation of 2QZ QSOs against SDSS EDR galaxies (in the NGC 2QZ strip) and APM galaxies (in the SGC 2QZ strip). The upper panel displays the cross-correlation signal for the 2 strips individually. The lower panel displays the signal combined for both strips. The lower panel shows estimates for both ‘directions’, centring on QSOs and counting galaxies ( $\omega_{qg}$ ) and centring on galaxies and counting QSOs ( $\omega_{gq}$ ). Error bars represent  $1\sigma$  jackknife errors. Labels note the number of objects of each population present within the confines of the 2QZ boundaries. Points within the same bin have been offset slightly for ease of display.

$\omega_{gg}$ , to  $\omega_{qg}$ , which shares the same random catalogue. It is useful, though, to have shown a significant, consistent anti-correlation between QSOs and galaxies irrespective of the ‘direction’ of the cross-correlation.

### 3.3 Is the Anti-Correlation Between Galaxies and QSOs a Selection Effect?

Certainly, there is a significant anti-correlation between galaxies and 2QZ QSOs. It is natural to ask if the signal arises when constructing the QSO or galaxy catalogues. There are several techniques that might produce an anti-correlation between QSOs and galaxies. The initial construction of the 2QZ UVX target catalogue removed extended images. Although all ‘high’ redshift ( $z \gtrsim 0.5$ ) QSOs should appear stellar, they may merge with foreground objects to look extended on images. A bright ( $b_j < 19.5$ ) subsample of these extended images should end up in the 2dF Galaxy Redshift Survey (henceforth 2dFGRS) and thus appear in deficit in the 2QZ. It turns out that this affects separations between galaxies and QSOs on scales of about 8 arcsec (Madgwick et al. 2002), smaller than the scales we are probing. Restrictions on the placement of 2dF fibres means the minimum angle between objects in a 2QZ field is about 30 arcsec, which might mean a paucity of objects at small separations. However, this restriction should not include QSO-galaxy separations as, although the 2QZ was carried out simultaneously with the 2dFGRS, QSO observations were given a higher observational priority, so we would expect few QSOs to be

rejected because of their proximity to galaxies. Additionally, the vast majority of fields in the 2dF survey were repeatedly observed to circumvent fibre-allocation problems. Myers et al. (2003) suggest that a 30 arcsec restriction on the minimum angle between 2dF objects in any field leaves no significant signature on these scales.

The easiest way to judge measurement systematics in the 2QZ is to consider a control sample of objects that underwent identical data reduction as the QSOs but should display no cosmological signatures. There are 10587 stars (with ‘11’ identification quality) in the 2QZ. In Fig. 5 we plot the cross-correlation of these stars against our galaxy samples. The upper panel of Fig. 5 compares the cross-correlation estimate for the NGC and SGC 2QZ strips. The agreement is reasonable, although the NGC sample is slightly more positively correlated with galaxies. Note that we might not expect the stellar correlation functions to be zero on all scales—gradients exist in local structure, which are not recreated in the random catalogues and which will make the correlation signal higher or lower on average. However, we would expect the stellar signature to be *flat* across the scales of interest. This is highlighted in the lower panel of Fig. 5, where we display the star-galaxy and galaxy-star cross correlations. Unlike in the QSO-galaxy case, there is a discrepancy in the large-scale zero-point of the correlation function that depends upon the ‘direction’ of the cross-correlation. As we might expect, when the random catalogue is constructed to match the stellar distribution, the zero-point of the correlation function drops significantly (to about -0.03). The large-scale value of the correlation function *is* zero when the random catalogue is constructed to match the galaxy distribution, which is free from (at least genuine physical) gradients. The key point, is that the correlation functions for stars and galaxies are flat (deviating at most  $0.5\sigma$  from their respective zero-points on scales larger than  $\theta \sim 0.4$  arcmin), indicating that systematics in the construction of the galaxy and QSO samples are low, hence induce no false correlations in our QSO-galaxy cross-correlations. The innermost points ( $\theta < 0.4$  arcmin) plotted in Fig. 5 seem to genuinely deviate from the zero-point and may be representative of merged images, fibre placement signatures or some other systematic. We will continue to plot these points in figures in this section but will not consider them in any modelling analysis or quotes of the significance of a signal.

### 3.4 Cosmological Explanations For the Anti-Correlation Between QSOs and Galaxies

An obvious physical effect, other than lensing, that could cause an anti-correlation between QSOs and galaxies is dust in galaxies obscuring background QSOs. This would lead to a dearth of QSOs around galaxies. Alternatively, if the anti-correlation *is* due to statistical lensing, we might be able to see the variation of the cross-correlation between galaxies and QSOs with the magnitude of the QSO sample.

#### 3.4.1 Is Intervening Dust the Cause of the Anti-Correlation Between QSOs and Galaxies?

We can use colour information to determine if intervening dust preferentially distributed around galaxies could

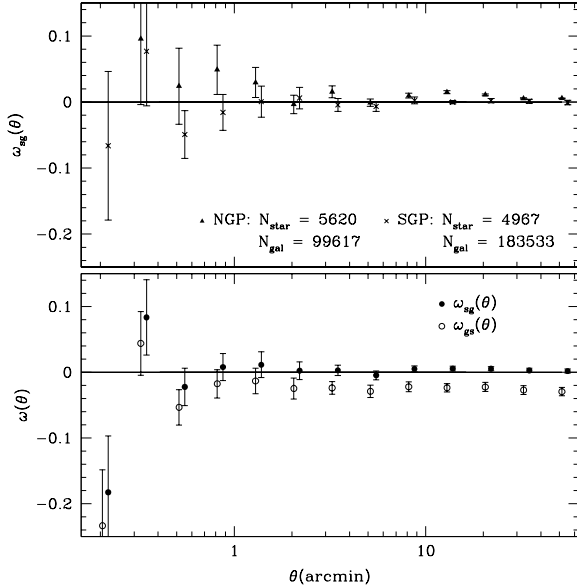


**Figure 5.** The cross-correlation of 2QZ stars against SDSS EDR galaxies (in the NGC 2QZ strip) and against APM galaxies (in the SGC 2QZ strip). The upper panel displays the cross-correlation signal for the 2 strips individually. The lower panel displays the signal combined for both strips. The lower panel shows estimates for both ‘directions’, centring on stars and counting galaxies ( $\omega_{sg}$ ) and centring on galaxies and counting stars ( $\omega_{gs}$ ). Error bars represent  $1\sigma$  jackknife errors. Labels note the number of objects of each population present within the confines of the 2QZ boundaries. Points within the same bin have been offset slightly for ease of display.

remove QSOs from the 2QZ catalogue out to 10 arcmin ( $\sim 1 h^{-1}\text{Mpc}$ ). Our method is similar to the correlation estimator of Equation 2 but instead of counting the average *number* of QSOs in differential annuli around galaxies, we work out the average *colour* of QSOs. Errors are calculated using 1000 bootstrapped simulations with the same QSO positions as the 2QZ catalogue but scrambled colours.

Knowing the expected QSO colour on degree scales, we can calculate the allowed colour excess,  $E(B-V)$ , in a given bin for both sets of measured 2QZ colours,  $u-b_j$  and  $b_j-r$ . Schlegel, Finkbeiner & Davis (1998) provide tables to convert from the colour excess to the amount of absorption by dust. Thus we can constrain the amount of dust around galaxies along QSO lines of sight.

Our  $1\sigma$  limits on absorption can be converted into a limit on the correlation function using a simple model outlined in Boyle, Fong & Shanks (1988). Dust around galaxies will cause an absorption (which we calculate from our measured colour excesses) that will alter the magnitude limit of the QSO number counts close to galaxies

$$\omega + 1 = \frac{N(< m)_{Gal}}{N(< m)_{Field}} = \frac{N(< m - A_{b_j})_{Field}}{N(< m)_{Field}} \quad (8)$$

where  $N(< m)$  is the integrated number counts,  $A_{b_j}$  is the absorption in the  $b_j$  band and the subscripts ‘Gal’ and ‘Field’ represent values near to galaxies and in the field, respectively. Equation 8 can easily be simplified if the number counts are represented by a power law but to be exact, we

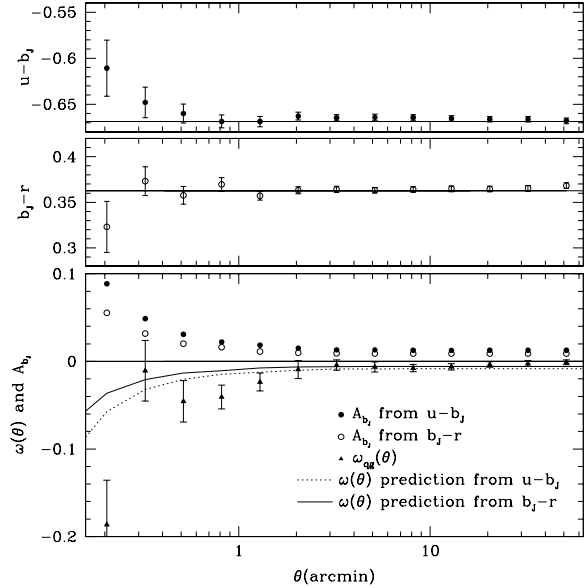


**Figure 6.** Limits on the amount of ‘typical’ dust that could account for the QSO-galaxy anti-correlation measured in Fig. 4. The upper panels show the average colour of QSOs in bins centred on SDSS EDR galaxies (in the NGC 2QZ strip) and APM galaxies (in the SGC 2QZ strip). Error bars in these panels represent the standard deviation ( $1\sigma$ ) in 1000 bootstrapped simulations with the same QSO positions as the 2QZ but scrambled colours. The lower panels translate these  $1\sigma$  error bars into limits on absorption in the  $b_j$  band ( $A_{b_j}$ ). The absorption limits are translated into limits on the QSO-galaxy cross-correlation using a simple model outlined in the text and displayed against the points and errors on  $\omega_{qg}$  from Fig. 4, represented by triangles.

will simply use the full fitted form of the number counts of 2QZ QSOs (see Fig. 1).

We now have a simple model that converts the error on our measurement of the average colour of QSOs near galaxies into a limit on the observed anti-correlation due to dust. In the upper two panels of Fig. 6, we show the average colour of QSOs around our galaxy samples with bootstrapped error bars, for 2QZ colours. A solid line marks the expected value from our scrambled bootstrap simulations. Except, perhaps, for the innermost bin, there is no significant deviation in the colour of QSOs from the expected value. The reddening displayed in the innermost bin of the  $u-b_j$  colours corresponds to an increase to the blue in the  $b_j-r$  colours, suggesting it is a small-scale measurement artefact or a statistical fluctuation, rather than due to dust. In the lower panel of Fig. 6, we translate the bootstrapped error bars into limits on absorption by dust around galaxies. The solid  $u-b_j$  and dashed  $b_j-r$  lines in the lower panel represent the  $1\sigma$  limit on the anti-correlation due to dust allowed by our colour limits. The anti-correlation between QSOs and galaxies measured in Fig. 4 is plotted for comparison. The  $1\sigma$  limits are insufficient to account for the anti-correlation between galaxies and QSOs, in fact, the  $b_j-r$  limits are marginally rejected, at a  $2\sigma$  level, and (at this level of rejection) could only account for about 30 per cent of the anti-correlation between QSOs and galaxies (out to 10 arcmin).

Schlegel, Finkbeiner & Davis (1998) base their absorption laws, from which our absorption estimates are de-

rived, on the difference in reddening between local, lightly-reddened standard stars and more distant reddened stars in the Milky Way (Cardelli, Clayton & Mathis 1989; O’Donnell 1994). The reddened stars are chosen to sample a wide range of interstellar environments (Fitzpatrick & Massa 1990) and Schlegel et al. demonstrate that their dust laws reproduce the reddening (as compared to the MgII index) of a sample of  $\sim 500$  elliptical galaxies that have broad sky coverage. However, by design, the absorption law used by Schlegel et al. only applies to our Galaxy. There is no reason to believe it is universal. In fact, though the Magellanic Clouds have been shown to have similar absorption laws to the Milky Way (Koornneef 1982; Bouchet et al. 1985), other local ( $z \lesssim 0.03$ ) galaxies have been shown to have ‘greyer’ absorption laws (Calzetti, Kinney, & Storchi-Bergmann 1994; Kinney et al. 1994), meaning that more dust absorption (approximately 25 per cent in the  $b_J$  band) is expected for the same reddening. At the  $2\sigma$  level, none of these alternative dust laws could provide enough absorption to explain the observed QSO-galaxy anti-correlation.

It is possible to construct dust models that would reconcile the lack of reddening of the QSO sample near galaxies with a paucity of QSOs around galaxies. For instance, the UVX QSO selection of the 2QZ means that QSOs that were excessively reddened may be lost entirely from the 2QZ, especially if the measured colours of 2QZ QSOs exhibit a large scatter around their intrinsic colours (which they don’t, at least at  $z < 2$  - see Croom et al. 2004). Also, if there was a lot of dust close to some galaxies, which completely obscured QSOs without reddening them, then the clustering of galaxies alone might lead to the observed galaxy-QSO anti-correlation. However, though various dust models can be constructed to explain a galaxy-QSO anti-correlation, it is very difficult to reconcile any dust model with the positive QSO-galaxy correlations seen in other samples (Williams & Irwin 1998; Gaztañaga 2003).

Acknowledging the provisos outlined above, we tentatively proceed assuming that dust around galaxies cannot account for the anti-correlation between QSOs and galaxies—but can we find definitive evidence that gravitational lensing is responsible?

### 3.4.2 *Dependence of the Cross-Correlation Signal on Magnitude and Redshift*

Perhaps the key prediction of magnification bias is that an enhancement of QSOs is expected near foreground lenses when the slope of the QSO number-magnitude counts is greater than 0.4 and a deficit of QSOs around the same lenses when the slope is less than 0.4. The QSO number counts are shown in Fig. 1. The ‘knee’ of the magnitude distribution, where the slope is 0.4, lies around  $b_J = 19.1$  to  $b_J = 19.6$ . A very simple model would predict (under the assumption that lensing samples QSOs up to about a magnitude fainter than the sample limit) a positive correlation between QSOs and galaxies up to a (QSO)  $b_J$  magnitude of around 18.1-18.6, no correlation between QSOs and galaxies in the range 18.1-18.6 to the knee of the magnitude counts, and an anti-correlation between QSOs and galaxies fainter than about  $b_J = 19.6$ .

At the time of writing, no author has yet shown the dependence of the cross-correlation signal with magnitude

from a positive correlation at bright QSO magnitudes to an anti-correlation at faint magnitudes, although some authors have shown the transition from a positive correlation to zero correlation (Williams & Irwin 1998; Gaztañaga 2003). This is mainly a problem of QSO sampling - as yet no single survey spans the QSO magnitude distribution in a manner that produces significant numbers of QSOs at both bright and faint magnitudes. The combined area and depth of the 2QZ and 6QZ allows us to trace the dependence of the cross-correlation between QSOs and galaxies with magnitude across the knee of the QSO number-magnitude counts for the first time. In the upper panel of Fig. 7 we show the dependence of the QSO-galaxy cross-correlation signal (measured out to 10 arcmin) in (differential) magnitude bins spanning the range  $16.25 < b_J < 20.85$ . QSOs are taken from the 2QZ for  $b_J > 18.25$  and from the 6QZ for  $b_J < 18.25$ . There is a loose trend in the data suggesting that the brightest QSOs are positively correlated with our galaxy samples (at the  $2.2\sigma$  level for  $b_J < 16.65$ ) and the faintest QSOs are anti-correlated with our galaxy samples (at the  $2.3\sigma$  level for  $b_J > 19.85$ ) and there is no significant result for the remainder of the magnitude range. To test whether this trend allows us to favour lensing over dust in foreground galaxies as a cause of the QSO-galaxy cross-correlation signal, we have constructed two toy models. The best-fitting models are displayed in Fig 7. The ‘dust’ model is essentially as shown in Equation 8 with  $A_{b_J}$ , the absorption (on 10 arcmin scales to match the data in Fig. 7) as the free parameter. The relative numbers in a given magnitude bin are calculated from the full integrated counts displayed in Fig. 1. The ‘lens’ model assumes that  $\omega_{qg} = K(2.5\alpha(m) - 1)$  where  $K$  is considered a constant (see Equation 15 below) out to the 10 arcmin scale of interest. There are actually two free parameters in this model,  $K$  and  $m$  where  $m$  is the number of magnitudes fainter than the bin of interest to sample the slope,  $\alpha$ , of the integrated number counts. The best dust model has  $A_{b_J} = 0.005$  with a reduced  $\chi^2$  value of 1.20 ( $P(\chi^2) = 0.29$ ). The best lens model has  $K = 0.015$ ,  $m = 2.1$  and a reduced  $\chi^2$  of 1.04 ( $P(\chi^2) = 0.41$ ). Neither of these simple models can be ruled out by the data. We cannot say with any confidence, then, that we have detected the full dependence of the cross-correlation signal with magnitude predicted by statistical lensing. This is not necessarily surprising, as there are very few objects in the 6QZ and only 256 QSOs brighter than  $b_J = 18.1$  that meet our usual redshift and identification quality selection criteria. Nevertheless, we do see a trend away from anti-correlations for brighter samples, in line with a lensing hypothesis.

In the lower panel of Fig. 7, we show the variation of the cross-correlation of 2QZ QSOs against our combined galaxy samples with redshift in differential bins of  $z = 0.4$ . A simple lensing model predicts no detectable trend in the cross-correlation signal with QSO redshift. We might expect a stronger signal at larger redshifts, as we will, on average, sample fainter QSOs in these bins and thus observe the signature of changes in magnitude in the redshift distribution. Indeed, we see a reasonably consistent anti-correlation for all redshift bins. The signal is slightly stronger at high redshifts but not significantly so. The lowest redshift QSOs are significantly correlated with our galaxy samples, no doubt due to genuine clustering at these redshifts, justifying our cut of  $z < 0.4$  in other analyses throughout this paper.



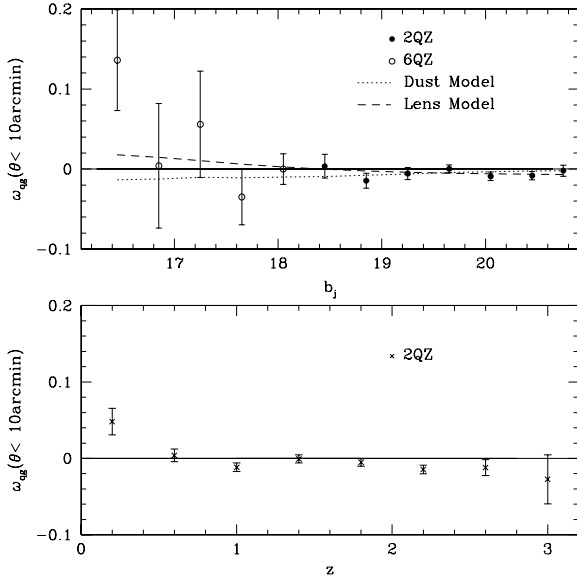


**Figure 7.** The cross-correlation of 2QZ QSOs against SDSS EDR galaxies (in the NGC 2QZ strip) and against APM galaxies (in the SGC 2QZ strip) and their dependence on  $b_J$  magnitude and redshift. The upper and lower panels display the cross-correlation signal measured out to 10 arcmin for subsamples of 2QZ and 6QZ QSOs in magnitude and redshift bins respectively. Error bars represent  $1\sigma$  jackknife errors. The ‘lensing’ and ‘dust’ models are described in the text.

In this section, we have shown a significant anti-correlation between faint QSOs and galaxies, and that is not a systematic effect of the QSO selection. We rule out the possibility that the majority of the signal is due to dust distributed around galaxies at the  $2\sigma$  level by comparing QSO colours in the field and close to galaxies, noting the caveat that models can be constructed where QSOs are obscured by dust without being reddened. We have shown that the anti-correlation is, however, consistent with lensing predictions. We will now model the anti-correlation assuming it is due to lensing and consider cosmological implications.

#### 4 STATISTICAL LENSING MODELS

In this section, we outline two lensing models we shall use in describing the anti-correlation between QSOs and galaxies. Both models compare the cross-correlation between QSOs and galaxies to the auto-correlation of galaxies to determine galaxy bias with respect to the mass traced by QSO light. The first, due to Williams & Irwin (1998; see also Williams & Frey 2003), uses a linear biasing prescription to relate fluctuations in the foreground mass distribution to QSO magnification. Williams & Irwin showed that this simple model agrees well with more complicated simulations (Dolag & Bartelmann 1997; Sanz, Martinez-Gonzalez & Benitez 1997). The second model, due to Gaztañaga (2003), allows for scale-dependent bias, and more fully considers the redshift distributions of the source and lens populations.

##### 4.1 Williams & Irwin Model

The convergence of lensing matter,  $\kappa$ , is defined as

$$\kappa(\theta) = \frac{\Sigma(D_l, \theta)}{\Sigma_{cr}(D_l, D_s)} \quad (9)$$

where  $\Sigma(D_l, \theta)$  is the surface mass density of the lensing material. The critical mass surface density is a function of the redshift of background source QSOs ( $z_s$ ) and of the foreground lensing matter ( $z$ ), and is defined

$$\Sigma_{cr}(D_l, D_s) = \frac{c^2}{4\pi G} \frac{D_s}{D_l D_{ls}} \quad (10)$$

for (angular diameter) lens distance  $D_l$ , source distance  $D_s$  and lens-source separation  $D_{ls}$ . We take  $z_s = 1.5$ , the median redshift of the 2QZ, for the background source redshift. Although this seems a rather extreme approximation of the actual distribution of QSOs, Bartelmann & Schneider (2001) suggest it is fair.

Williams & Irwin model the lensing material as a smooth slab that extends over the redshift range  $z = 0$  to  $z = z_{\max} = 0.3$ , where the extent of the redshift distribution is estimated using the magnitude-redshift selection function of Baugh & Efstathiou (1993), which provides a good fit (Maddox et al. 1996) to the Stromlo-APM Survey redshift distribution (Loveday et al. 1992a; Loveday et al. 1992b). We will also use the selection function of Baugh & Efstathiou to model the galaxy redshift distribution. Note that just over 95 per cent of galaxies are included out to  $z_{\max} = 0.3$ .

Lensing arises due to angular fluctuations in the projected matter density around the mean. The mass fluctuations can be characterised by the density contrast  $\delta(\theta)$ , which measures the mass density at a given scale relative to the mean across the sky. As the density across the entire sky is the mean, the distribution of density contrast is normalised ( $\int P(\delta|\theta)\delta d\delta = 1$ ). The effective lensing convergence due to mass fluctuations are enhanced above the mean, yielding  $\kappa_{\text{eff}}(\theta) = \bar{\kappa}(\delta - 1)$ . In this model, bias is scale-independent, meaning that galaxy fluctuations trace mass fluctuations as  $\delta_G(\theta) - 1 = b[\delta(\theta) - 1]$ . The surface density of a slab of matter of thickness  $cdt$  at redshift  $z$ , is  $\Sigma = \rho_{crit}\Omega_0(1+z)^3 cdt$ , where  $\rho_{crit}$  is the critical density of the Universe. Thus

$$\kappa_{\text{eff}}(\theta) = \frac{\bar{\kappa}}{b}(\delta_G - 1) = \frac{3H_0^2 c \Omega_0}{8\pi G} \frac{\Omega_0}{b} (\delta_G - 1) \int_0^{z_{\max}} \frac{(1+z)^3 \frac{dt}{dz} dz}{\Sigma_{cr}(z, z_s)} \quad (11)$$

The enhancement of QSO number density over the mean around any galaxy is given, for QSO number-counts with slope  $\alpha$ , by

$$\delta_Q = \mu^{2.5\alpha-1} \approx \left(1 + 2\bar{\kappa} \frac{(\delta_G - 1)}{b}\right) (2.5\alpha - 1) \quad (12)$$

where  $\mu \approx 1 + 2\kappa_{\text{eff}}$  is the lensing magnification in the weak regime (and we’ve performed a Taylor Expansion). Now, the QSO-galaxy cross-correlation can be estimated by the enhancement in galaxy counts across the probability distribution of galaxy density contrasts

$$\omega_{qg}(\theta) + 1 = \int P(\delta_G|\theta) \delta_G \delta_Q d\delta_G \quad (13)$$

substituting Equation 12 into the previous equation and remembering  $\int P(\delta|\theta)\delta d\delta = 1$ , one can rearrange to show

$$\omega_{qg}(\theta) = (2.5\alpha - 1) \frac{2\bar{\kappa}}{b} \left[ \int P(\delta_G|\theta)\delta_G d\delta_G \right] - 1 \quad (14)$$

so, finally

$$\omega_{qg}(\theta) = (2.5\alpha - 1) \frac{2\bar{\kappa}}{b} \omega_{gg}(\theta) \quad (15)$$

relates  $\omega_{qg}(\theta)$ , to  $\omega_{gg}(\theta)$  and  $b$ , the (scale-independent) bias parameter. Other than  $b$ , cosmology is contained in the (dimensionless) mean convergence  $\bar{\kappa}$  (Equation 11). The QSO number counts are included in the power-law slope,  $\alpha$ .

## 4.2 Gaztañaga Model

This model is reviewed in the Appendix, and described in detail by Gaztañaga (2003; see also Myers 2003). Gaztañaga (2003) has shown that a good power-law expression for scale-dependent biasing of galaxies is

$$b(R) = b_{0.1} \left( \frac{0.1 h^{-1} \text{Mpc}}{R} \right)^{\gamma_b} \quad (16)$$

Whilst Gaztañaga assumed that this bias corresponded to the ratio of the galaxy and matter correlation functions (see also Guimãraes 2001);  $b(r) = [\xi_{gg}(r)/\xi_{mm}(r)]^{0.5}$ , we are in fact comparing the cross-correlation of QSOs and galaxies with the galaxy auto-correlation function, and so are defining a bias function via  $b(r) = \xi_{gg}(r)/\xi_{gm}(r)$ . Whilst on large scales these two definitions should be equal, one expects the halo of the central galaxy to affect the shape of  $\xi_{gm}(r)$  on small scales. Therefore we consider a revised version of the Gaztañaga model to take this into account.

Through observation of  $\omega_{gg}$  and  $\omega_{gq}$  we can constrain the amplitude and slope of the bias correlation function. The two-dimensional projection of the galaxy correlation function is (consider Peebles 1980)

$$\omega_{gg}(\theta) = \sigma_{0.1}^2 b_{0.1} b^* \theta^{1-\gamma_{gg}} A_{gg,0.1} \quad (17)$$

whilst the galaxy-QSO cross-correlation is given by

$$\omega_{gq}(\theta) = \sigma_{0.1}^2 b^* \theta^{1-\gamma_{gq}} A_{gq,0.1} \quad (18)$$

where  $\sigma_{0.1}$ , the amplitude of fluctuations in the matter correlation function (averaged over a sphere of radius  $0.1 h^{-1} \text{Mpc}$ ) is defined in Equation A3,  $A_{gg,0.1}$  and  $A_{gq,0.1}$  depend on the radial selection functions of the galaxy and QSO samples and the lensing efficiency, and  $b$  and  $\gamma$  denote the slope and amplitude of a scale-dependent bias model. In the particular case where the two bias definitions ( $[\xi_{gg}/\xi_{gm}]$ ;  $[\xi_{gg}/\xi_{mm}]^{0.5}$ ) are equivalent,  $b^*$  is equivalent to  $b_{0.1}$  (see the Appendix for further details on these parameters, particularly  $b^*$ ).

The slope of the bias correlation function,  $\gamma_b$ , can be easily determined from  $\gamma_{gg}$  and  $\gamma_{gq}$ . The bias parameter,  $b_{0.1}$ , can then be determined

$$b_{0.1} = \frac{\omega_{gg}(\theta) A_{gq,0.1} \theta^{\gamma_b}}{\omega_{gq}(\theta) A_{gg,0.1}} \quad (19)$$

In the case where the two bias definitions, above, agree exactly (as implicitly assumed by Gaztañaga),  $b^* = b_{0.1}$  and

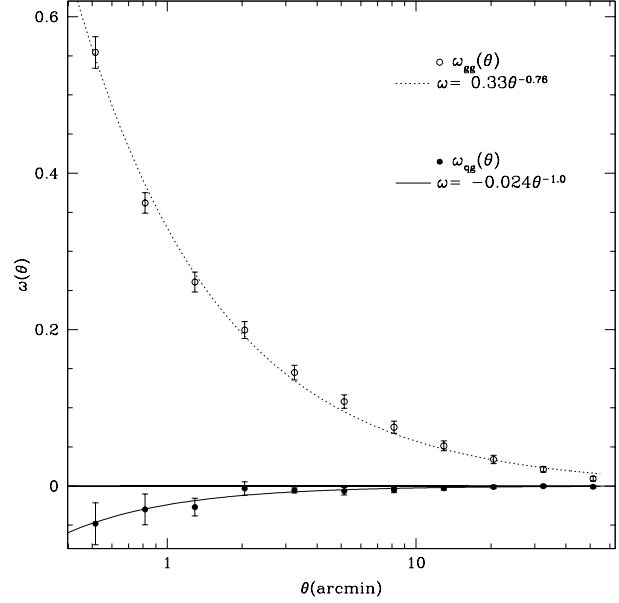


**Figure 8.** The galaxy-galaxy auto-correlation combined from SDSS EDR galaxies (in the NGC strip) and APM galaxies (in the SGC strip) is compared to the faint-end QSO-galaxy cross-correlation function. Both correlation functions are fitted by power laws, displayed by lines drawn through the respective data. Error bars represent  $1\sigma$  jackknife errors.

$\gamma^* = \gamma_b$ . In this case, one can further derive the slope of the mass correlation function,  $\gamma$ , and  $\sigma_{0.1}$  can be determined via

$$\sigma_{0.1}^2 = \frac{\omega_{gq}(\theta)^2 A_{gg,0.1} \theta^{\gamma-1}}{\omega_{gg}(\theta) A_{gq,0.1}^2} \quad (20)$$

## 5 RESULTS AND DISCUSSION

In Fig. 8 we plot the auto-correlation of galaxies combined for galaxies from the SDSS EDR in the NGC 2QZ strip and the APM Survey in the SGC 2QZ strip. Fig. 8 also shows the anti-correlation between QSOs and galaxies discussed throughout this paper. We have plotted the result for the QSO sample fainter than  $b_J = 19.6$ , to ensure we are sampling QSOs from a region of the number-magnitude counts fainter than the ‘knee’ of the distribution (see Section 3.4.2). We fit simple power-laws to the two correlation functions, finding that

$$\omega_{qg}(\theta) = -0.024 \pm_{0.007}^{0.008} \theta^{-1.0 \pm 0.3} \quad (21)$$

$$\omega_{gg}(\theta) = 0.330 \pm_{0.014}^{0.015} \theta^{-0.76 \pm 0.04} \quad (22)$$

where  $\theta$  is expressed in arcminutes, 1 arcminute being about  $0.1 h^{-1} \text{Mpc}$  at the median redshift of our galaxy data. In both cases, a simple  $\chi^2$  fit suggests good power-law approximations to the data, with a reduced  $\chi^2$  value of 1.6 ( $P(\chi^2) = 0.11$ ) for the galaxy-galaxy correlation fit and 1.4 ( $P(\chi^2) = 0.20$ ) for the QSO-galaxy anti-correlation fit. The result for the slope of the galaxy-galaxy auto-correlation is in excellent agreement with recent small-scale measurements for galaxies with similar limiting flux to the sample used here (Connolly et al. 2002).

Model		$\Omega_m = 0.3, \Omega_\Lambda = 0.7$	$\Omega_m = 1$
W&I, 98	$b_{0.1}$	$0.13 \pm_{0.07}^{0.08}$	$0.32 \pm_{0.18}^{0.20}$
Gaz, 03	$b_{0.1}$	$0.052 \pm_{0.027}^{0.064}$	$0.142 \pm_{0.072}^{0.167}$
	$b_{0.2}$	$0.061 \pm_{0.025}^{0.055}$	$0.166 \pm_{0.069}^{0.144}$

**Table 1.** In the row labelled ‘W&I, 98’ we list  $b$ , evaluated at  $\theta = 1$  arcmin ( $\sim 0.1 h^{-1}$ Mpc), as measured from Equation 23, with  $\Sigma_{cr}(z, z_s)$  calculated using Equation 10 with  $z_s = 1.5$  for the median QSO redshift. In the row labelled ‘Gaz, 03’ we list  $b$  evaluated at  $\theta = 1$  arcmin, and  $\theta = 2$  arcmin ( $\sim 0.2 h^{-1}$ Mpc), as measured from Equation 19. Both estimates are shown for  $\Lambda$ CDM and EdS cosmological models, assuming  $H_0 = 70 \text{ km s}^{-1} \text{ Mpc}^{-1}$ .

### 5.1 Williams & Irwin Model

Taking our measured values for the correlation functions, evaluated at  $\theta = 1$  arcmin ( $\sim 0.1 h^{-1}$ Mpc), and a faint end slope of  $\alpha = 0.29 \pm 0.03$ , Equation 15 (Williams & Irwin 1998) reduces to

$$b_{0.1} = 7.56 \pm_{4.24}^{4.83} \bar{\kappa}, \quad (23)$$

a function of the convergence,  $\bar{\kappa}$ . We calculate this assuming either an Einstein-de-Sitter (henceforth EdS), or  $\Lambda$ CDM cosmology, and the resulting values of  $b$  are displayed in Table 1. The model is somewhat dependent on the parameter  $z_{\text{max}}$  of Equation 11. For instance, increasing  $z_{\text{max}}$  from 0.3 to 0.4 increases the estimates of  $b_{0.1}$  by 50 per cent, with the errors scaling accordingly. In our samples, 99.5 per cent of galaxies lie at  $z < 0.4$ .

Note that, as the measured slopes of  $\omega_{gg}(\theta)$  and  $\omega_{gq}(\theta)$  are not the same, a scale-independent model of bias is only marginally accepted. It is relatively easy to extend Equation 15 to a simple model of scale-dependent bias, obtaining

$$b = b_{0.1} \left( \frac{0.1 h^{-1} \text{Mpc}}{r} \right)^{-0.24 \pm 0.30}, \quad (24)$$

where  $b_{0.1}$  is shown in Table 1 and  $r$  is equivalent to  $\theta$  expressed in  $h^{-1}$ Mpc at the mean redshift of our galaxy data.

### 5.2 Gaztañaga Model

Using the measured slopes  $\gamma_{gg}$  and  $\gamma_{gq}$ , we find a slope for the bias correlation function of  $\gamma_b = -0.24 \pm 0.30$ . We now use Equation 19 to determine the galaxy bias in both  $\Lambda$ CDM and EdS cosmologies, with  $H_0 = 70 \text{ km s}^{-1} \text{ Mpc}^{-1}$ , for  $0.1 h^{-1}$ Mpc scales. The results are displayed in Table 1. The analysis is repeated measuring  $b$  on  $0.2 h^{-1}$ Mpc scales to allow a direct comparison with the results of Gaztañaga (2003). The results only have a slight dependence on  $H_0$ . Increasing  $H_0$  to  $100 \text{ km s}^{-1} \text{ Mpc}^{-1}$  increases the estimate of  $b$  by 9 per cent (for both EdS and  $\Lambda$ CDM cosmologies, and for both  $b_{0.1}$  and  $b_{0.2}$ ). Decreasing  $H_0$  to  $50 \text{ km s}^{-1} \text{ Mpc}^{-1}$  decreases  $b$  by either 8 per cent ( $\Lambda$ CDM) or 7 per cent (EdS).

Using the fit to  $\omega_{gg}(\theta)$  from Equation 22, together with Equation 19, we derive a model for  $\omega_{gq}(\theta)$  as a function of  $b_{0.1}$  and  $\gamma_b$ . We fit this model to the cross-correlation data by performing a maximum likelihood analysis, determining the likelihood of each model by calculating the  $\chi^2$  value of each fit. Fig. 9 shows likelihood contours in the  $b_{0.1} - \gamma_b$

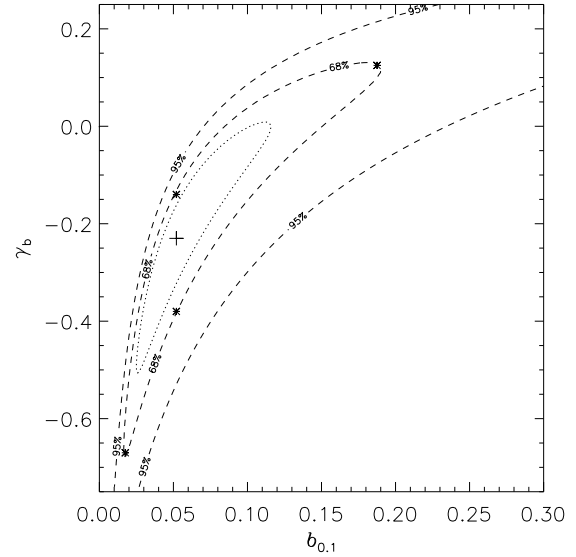


**Figure 9.** Likelihood contours in the  $b_{0.1} - \gamma_b$  plane for a fit to the QSO-galaxy cross-correlation function,  $\omega_{gq}(\theta)$ , assuming  $\Lambda$ CDM. Contours are plotted for  $\chi^2$  values corresponding to a one-parameter confidence of 68 per cent (dotted contour), and two-parameter confidence of 68 and 95 per cent (dashed contours). The best fit model obtained (marked with a +) has  $b_{0.1} = 0.052$  and  $\gamma_b = -0.23$ . The stars mark the models plotted with dashed lines in Figure 10.

$\gamma_b$  plane. There is a clear degeneracy, with stronger scale-dependence of bias (i.e. more negative  $\gamma_b$ ) implying a lower value of  $b_{0.1}$ . The uncertainty in our determination of  $b$  is somewhat larger than the quoted error in Gaztañaga (2003), and, as demonstrated by Fig. 9, is considerably skewed in  $b$ -space. From Fig. 9 it is possible to reconcile the value of  $b_{0.1}$  obtained with the method of Gaztañaga with the somewhat higher value of  $b_{0.1}$  obtained using the Williams & Irwin model: the latter assumes scale-invariant bias, or  $\gamma_b = 0$ , which corresponds to a higher value of  $b_{0.1} \sim 0.12$  from the  $b_{0.1} - \gamma_b$  degeneracy in the Gaztañaga model fit.

### 5.3 Discussion

It is interesting that our bias predictions, based on a detection of a galaxy-QSO *anti*-correlation, agree well with the predictions of an independent author (Gaztañaga 2003) who reported a *positive* galaxy-QSO correlation, working with bright QSOs and (mostly) independent data. Both of the methods we have used in this paper, which use quite different lensing models to determine the amplitude of the galaxy bias parameter,  $b$ , consistently agree that on scales of  $0.1 h^{-1}$ Mpc, galaxies are strongly anti-biased (i.e.  $b < 1$ ) with a bias parameter of  $b \sim 0.1$ . Using a simple model (Williams & Irwin 1998) and assuming that lensing matter can be represented by a uniform slab extending out to the redshift where 95 per cent of the surveyed galaxies are included, and the lensed QSOs may be represented by a single population at  $z = 1.5$ , we find  $b_{0.1} = 0.13 \pm_{0.07}^{0.08}$  for a  $\Lambda$ CDM cosmology. A more realistic model that traces spherical fluctuations in the underlying lensing matter on

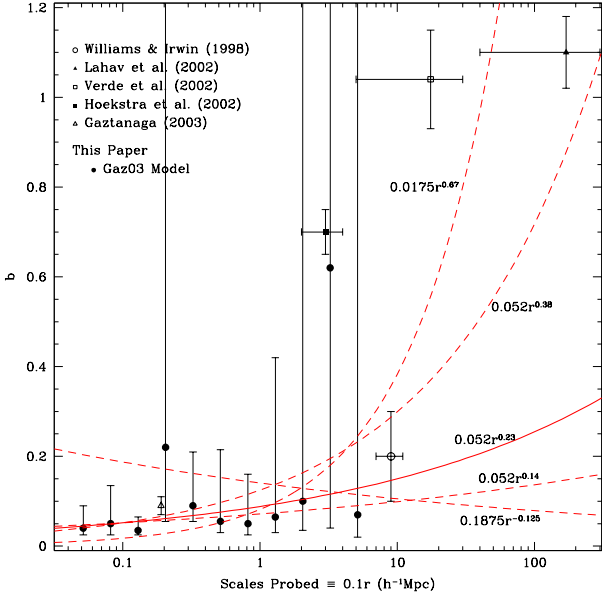


**Figure 10.** A comparison of some recent measurements of the bias parameter with those made in this paper. The filled circles are measurements of the bias parameter deduced from the ratio of the correlation functions in Fig. 8 using Equation 19 (i.e. the ‘Gaztañaga Model’). The angular bins of the correlation functions have been projected to the median redshift of the galaxy distribution ( $z \sim 0.12$ ). The solid line represents the best fitting bias model, with  $b_{0.1} = 0.052$  and  $\gamma_b = -0.23$ . The various dashed lines depict the error ranges taken from the 68% likelihood contour; the models chosen are shown by stars in Figure 9. Each measurement displayed from this paper is calculated using a  $\Lambda$ CDM cosmology. Other points represent recent measurements of the bias parameter from the literature.

$0.1 h^{-1}$  Mpc scales, across the redshift distributions of our QSO and galaxy samples (Gaztañaga 2003), yields  $b_{0.1} = 0.04 \pm_{0.01}^{0.18}$ . Note that, whilst traditionally galaxy bias is measured from the ratio between the galaxy auto-correlation and the mass auto-correlation, as we are comparing the cross-correlation of QSOs and galaxies with the galaxy auto-correlation function, we are instead defining a bias function via  $b(r) = \xi_{gg}(r)/\xi_{gm}(r)$ .

A value of  $b \sim 0.1$  might seem at odds with observations of much higher values of  $b \sim 1$  on Megaparsec scales (Verde et al. 2002; Lahav et al. 2002; Hoekstra et al. 2002), assuming a simple linearly-biased  $\Lambda$ CDM mass distribution, suggesting more mass around galaxies than expected. However, the slope of the scale-dependent bias parameter is found to be  $\gamma_b = -0.24 \pm 0.3$ . Although we cannot rule out a linear bias parameter on scales of  $0.1 h^{-1}$  Mpc from the slopes of our fitted correlation functions, the fact that many other authors determine much higher values of  $b \sim 1$  on Megaparsec scales (Verde et al. 2002; Lahav et al. 2002; Hoekstra et al. 2002) suggests that bias might be a strong function of scale on  $100 h^{-1}$  kpc scales. In Fig. 10 we plot the bias implied across a range of scales from measurements made in this paper and compare them to measurements made by other authors (Williams & Irwin 1998; Verde et al. 2002; Lahav et al. 2002; Hoekstra et al. 2002; Gaztañaga 2003). The models discussed in this paper allow a scale-dependent model (with  $b \sim r^{0.5}$ ) that is consistent both with our ob-

servations on  $0.1 h^{-1}$  Mpc scales, as well as other measures of the galaxy bias parameter, with  $b \sim 1$ , on larger scales (Lahav et al. 2002; Verde et al. 2002). Whilst the models shown in Fig. 10 appear inconsistent with the measurements of Hoekstra et al. (2002), it may be that the simple model of scale-dependent bias assumed (equation 16) is not a good description of bias on larger scales. Indeed, on very large scales, bias is expected to be linear and hence independent of scale. On the other hand, Williams & Irwin (1998) suggest galaxies are highly anti-biased ( $b \sim 0.1$ ) even on  $5\text{--}10 h^{-1}$  Mpc scales, which would only be consistent with our observations if bias has no scale-dependence and is certainly inconsistent with the results of other authors (Lahav et al. 2002; Verde et al. 2002; Hoekstra et al. 2002).

To attempt to explain strong scale-dependence of bias, and, therefore, a higher than expected galaxy-mass cross-correlation signal on  $100 h^{-1}$  kpc scales, we can consider halo occupation models of the galaxy distribution (Berlind & Weinberg 2002; Jain et al. 2003). The form of the cross-correlation in a  $\Lambda$ CDM universe can be determined from simulations, using halo occupation models to populate dark matter haloes with galaxies (Berlind & Weinberg 2002; Jain et al. 2003), and taken in ratio with the real-space galaxy auto-correlation function measured from the APM galaxy catalogue (Baugh 1996), such models typically yield a value of  $b \sim 0.6$  on  $0.1 h^{-1}$  Mpc scales. Thus some level of anti-bias arises naturally in halo occupation models (albeit not as much as observed), going some way towards explaining the discrepancy. However, these models are complicated and depend strongly on galaxy type, and are thus not well constrained on the scales probed. Whilst a high QSO-galaxy cross-correlation signal places a constraint on such models, it may be possible to reconcile them with a better understanding of how galaxies populate haloes.

By comparing the two definitions ( $[\xi_{gg}/\xi_{gm}]$  and  $[\xi_{gg}/\xi_{mm}]^{0.5}$ ) of  $b(r)$  in a range of simulations, Berlind and Weinberg (2002) demonstrated that whilst they are not in perfect agreement in the scale-dependent bias regime ( $0.1 < r < 4 h^{-1}$  Mpc), the two definitions of  $b(r)$  have a very similar shape over this range. However, given the large anti-bias found, and strong scale-dependence of bias implied, it is quite likely that they *will in fact be considerably different*. Therefore, care needs to be taken in interpreting the results of this analysis. In particular, we have chosen not to follow the analysis of Gaztañaga (2003) in deriving the slope of the mass correlation function,  $\gamma$ , and  $\sigma_{0.1}$  under the assumption that the two bias definitions are equal, as it is likely that this would lead to a large systematic error, and hence misleading results.

Finally we should point out that in this work we have assumed the weak lensing approximation,  $\mu \approx 1 + 2\kappa$ . Takada and Hamana (2003) have shown that a non-linear magnification correction will enhance the amplitude of the magnification correlation by around 10–25 per cent on arcminute scales for the QSO-galaxy cross-correlation signal, and such a correction would therefore boost our bias estimates by this fraction. Whilst in the right direction, such a correction is too small to explain the observed discrepancy in a  $\Lambda$ CDM cosmology. Note also that Table 1 indicates that an EdS cosmology with a value of  $b_{0.1} \sim 1$  agrees with the data at the  $2\sigma$  level. Though an EdS framework is consistent with the previous QSO lensing results of Croom & Shanks (1999)

and Myers et al. (2003), it is inconsistent with the majority of recent cosmological data.

## 6 CONCLUSIONS

In this paper, we have studied the cross-correlation of galaxies and background QSOs. Galaxies were drawn from the APM Survey in the region of the 2dF QSO Redshift Survey Southern Galactic Cap strip and the Sloan Digital Sky Survey Early Data Release in the Northern Galactic Cap strip. The QSO-galaxy cross-correlation function  $\omega_{gq}$  suggests that 2QZ QSOs and galaxies are anti-correlated with significance ( $2.8\sigma$ ) and strength  $-0.007$ , over the angular range out to 10 arcmin ( $1 h^{-1}\text{Mpc}$  at the median redshift of our galaxy samples). This result is unique in that it is possibly the first significant anti-correlation detected between QSOs and galaxies that is not subject to small sample sizes or problems in selecting the populations.

Our detection of a galaxy-QSO anti-correlation is consistent with the predictions of statistical lensing theory. When combined with the work of Gaztañaga (2003), a consistent picture emerges that spans faint and bright QSO samples, which, due to the changing QSO number-magnitude count slope, have very different clustering properties, relative to the foreground galaxy population.

We have also considered a number of other possible explanations for the anti-correlation between QSOs and galaxies. Firstly, errors and the correlation estimator were proven robust against Monte Carlo simulations. Care was taken to demonstrate that there is no significant correlation ( $0.5\sigma$  positive correlation) between stars (which were selected within the 2dF Survey in the same way as the QSO sample) and our galaxy samples. We are thus confident that the anti-correlation between QSOs and galaxies is not a systematic error. The colours of QSOs around galaxies were used to place limits on the effect dust (modelled with an absorption law appropriate to the Milky Way) could have in producing an anti-correlation of QSOs with galaxies. Whilst our simple dust models could account for at most a third of the observed anti-correlation signal (at  $2\sigma$  significance), we do not rule out the possibility that scatter in QSO colours might preferentially discard reddened QSOs from the 2QZ, nor do we specifically rule out dust models that could obscure QSOs without reddening them, such as grey dust, or heavy concentrations of dust in some galaxies. No dust model, however, could easily explain the positive galaxy-QSO correlations found by Gaztañaga (2003).

We find that, for a  $\Lambda\text{CDM}$  cosmology, galaxies are highly anti-biased on small scales. We consider two models that use quite different descriptions of the lensing matter and find they yield consistent predictions for the strength of galaxy bias on  $0.1 h^{-1}\text{Mpc}$  scales of  $b \sim 0.1$ . The inferred strength of this result is in agreement with the work of Gaztañaga (2003). The slope of the scale-dependent bias parameter is found to be  $\gamma_b = -0.24 \pm 0.3$ . The fact that many other authors determine much higher values of  $b \sim 1$  on Megaparsec scales (Verde et al. 2002; Lahav et al. 2002; Hoekstra et al. 2002) suggests that bias might be a strong function of scale.

To explain such strong scale-dependence of bias, we can consider halo occupation models of the galaxy distribution

(Berlind & Weinberg 2002; Jain et al. 2003). Such models predict some level of anti-bias on  $0.1 h^{-1}\text{Mpc}$  scales, typically yielding a value of  $b \sim 0.6$  (Berlind & Weinberg 2002). However, these models are complicated and depend strongly on galaxy type, and are thus not well constrained on the scales probed. Therefore, it may be possible to reconcile them with the observations reported here through a better understanding of how galaxies populate haloes.

An alternative interpretation of these results is that they indicate that there is significantly more mass present, at least on the  $100 h^{-1}\text{kpc}$  scales probed, than predicted by  $\Lambda\text{CDM}$ . Myers et al. (2003) recently detected a strong anti-correlation between the same faint 2QZ QSOs and groups of galaxies. By applying models of gravitational lensing by simple haloes they used this anti-correlation signal to determine the mass of these lensing galaxy groups, concluding that the observed anti-correlation favours considerably more mass in groups of galaxies than accounted for in a universe with density parameter  $\Omega_m = 0.3$ . It is hard to account for the statistical lensing properties either of the galaxies presented here, or the groups of galaxies from Myers et al., in a low mass ( $\Omega_m \sim 0.3$ ) universe with scale-independent bias.

## ACKNOWLEDGEMENTS

The 2dF QSO Redshift Survey was based on observations made with the Anglo-Australian Telescope and the UK Schmidt Telescope, and we would like to thank our colleagues on the 2dF Galaxy Redshift Survey team and all the staff at the AAT that have helped to make this survey possible. ADM acknowledges the support of a PPARC studentship. PJO acknowledges the support of a PPARC Fellowship. This work was partially supported by the ‘SISCO’ European Community Research and Training Network.

Funding for the creation and distribution of the SDSS Archive has been provided by the Alfred P. Sloan Foundation, the Participating Institutions, the National Aeronautics and Space Administration, the National Science Foundation, the U.S. Department of Energy, the Japanese Monbukagakusho, and the Max Planck Society. The SDSS Web site is <http://www.sdss.org/>.

The SDSS is managed by the Astrophysical Research Consortium (ARC) for the Participating Institutions. The Participating Institutions are The University of Chicago, Fermilab, the Institute for Advanced Study, the Japan Participation Group, The Johns Hopkins University, Los Alamos National Laboratory, the Max-Planck-Institute for Astronomy (MPIA), the Max-Planck-Institute for Astrophysics (MPA), New Mexico State University, University of Pittsburgh, Princeton University, the United States Naval Observatory, and the University of Washington.

## REFERENCES

- Bartelmann M., 1995, *A&A*, 298, 661
- Bartsch A., Schneider P., Bartelmann M., 1997, *A&A*, 319, 375
- Bartelmann M., Schneider P., 2001, *PhR*, 340, 291
- Baugh C. M., Efstathiou G., 1993, *MNRAS*, 265, 145
- Baugh C. M., 1996, *MNRAS*, 280, 267
- Benitez N., Martinez-Gonzalez E., 1997, *ApJ*, 477, 27
- Berlind A. A., Weinberg D. H., 2002, *ApJ*, 575, 587

Bernardeau F., van Waerbeke L., Mellier Y., 1997, *A&A*, 322, 1  
 Bouchet P., Lequeux J., Maurice E., Prevot L., Prevot-Burnichon M. L., 1985, *A&A*, 149, 330  
 Boyle B. J., Fong R., Shanks T., 1988, *MNRAS*, 231, 897  
 Calzetti D., Kinney A. L., Storchi-Bergmann T., 1994, *ApJ*, 429, 582  
 Cardelli J. A., Clayton G. C., Mathis J. S., 1989, *ApJ*, 345, 245  
 Carlberg R. G., Yee H. K. C., Morris S. L., Lin H., Hall P. B., Patton D., Sawicki M., Shepherd C. W., 2000, *ApJ*, 542, 57  
 Connolly A. J., et al., 2002, *ApJ*, 579, 42  
 Croom S. M., Shanks T., 1996, *MNRAS*, 281, 893  
 Croom S. M., Shanks T., 1999, *MNRAS*, 307, L17  
 Croom S. M., Smith R. J., Boyle B. J., Shanks T., Miller L., Outram P. J., Loaring N. S., 2004, *MNRAS*, 349, 1397  
 Dolag K., Bartelmann M., 1997, *MNRAS*, 291, 446  
 Ferreras I., Benitez N., Martinez-Gonzalez E., 1997, *AJ*, 114, 1728  
 Fitzpatrick E. L., Massa D., 1990 *ApJS*, 72, 163  
 Fugmann W., 1990, *A&A*, 240, 11  
 Gaztañaga E., 2003, *ApJ*, 589, 82  
 Groth M. G., Peebles P. J. E., 1977, *ApJ*, 217, 385  
 Guimãraes A. C. C., van De Bruck C., Brandenberger R. H., 2001, *MNRAS*, 325, 278  
 Hamilton A. J. S., Kumar P., Lu E., Matthews A., 1991, *ApJ*, 374, 1  
 Hamilton A. J. S., 1993, *ApJ*, 417, 19  
 Hoekstra H., van Waerbeke L., Gladders M. D., Mellier Y., Yee H. K. C., 2002, *ApJ*, 577, 604  
 Jain B., Scranton R., Sheth R. K., 2003, *MNRAS*, 345, 62  
 Kaiser N., 1984, *ApJ*, 284, 9  
 Kinney A. L., Calzetti D., Bica E., Storchi-Bergmann T., 1994, *ApJ*, 429, 172  
 Koornneef J., 1982, *A&A*, 107, 247  
 Kovner I., 1989, *ApJ*, 341, 1  
 Lahav O., et al., 2002, *MNRAS*, 335, 432  
 Landy S. D., Szalay A. S., 1993, *ApJ*, 412, 64  
 Loveday J., Peterson B. A., Efstathiou G., Maddox S. J., 1992a, *ApJ*, 390, 338  
 Loveday J., Efstathiou G., Peterson B. A., Maddox S. J., 1992b, *ApJ*, 400, 43  
 Maddox S. J., Efstathiou G., Sutherland W. J., 1990a, *MNRAS*, 246, 433  
 Maddox S. J., Efstathiou G., Sutherland W. J., Loveday J., 1990b, *MNRAS*, 243, 692  
 Maddox S. J., Efstathiou G., Sutherland W. J., 1996, *MNRAS*, 283, 1227  
 Madgwick D. S., Hewett P. C., Mortlock D. J., Lahav O., 2002, *MNRAS*, 334, 209  
 Menard B., Bartelmann M., 2002, *A&A*, 386, 784  
 Myers A. D., 2003, PhD Thesis, University of Durham  
 Myers A. D., Outram P. J., Shanks T., Boyle B. J., Croom S. M., Loaring, N. S., Miller L., Smith R. J., 2003, *MNRAS*, 342, 467  
 Narayan R., 1989, *ApJ*, 339, 53  
 Norberg P., et al., 2002, *MNRAS*, 332, 827  
 Norman D. J., Williams L. L. R., 2000, *AJ*, 118, 613  
 O'Donnell J. E., 1994, *ApJ*, 422, 158  
 Outram P. J., Hoyle F., Shanks T., Croom S. M., Boyle B. J., Miller L., Smith R. J., Myers A. D., 2003, *MNRAS*, 342, 483  
 Peacock J. A., Dodds S. J., 1994, *MNRAS*, 267, 1020  
 Peebles P. J. E., 1980, in *The Large Scale Structure in the Universe*, Princeton University Press, ISBN 0-691-08240-5  
 Phillipps S., Fong R., Fall R. S., Ellis S. M., MacGillivray H. T., 1978 *MNRAS*, 182, 673  
 Sanz J. L., Martinez-Gonzalez E., Benitez N., 1997, *MNRAS*, 291, 418  
 Schlegel D. J., Finkbeiner D. P., Davis M., 1998, *ApJ*, 500, 525  
 Schneider P., 1989, *A&A*, 221, 221  
 Scranton R., et al., 2002, *ApJ*, 579, 48

Seldner M., Peebles P. J. E., 1979, *ApJ*, 227, 30  
 Shanks T., Boyle B. J., 1994, *MNRAS*, 271, 753  
 Stevenson P. R. F., Shanks T., Fong R., MacGillivray H. T., 1985, *MNRAS*, 213, 953  
 Stoughton C., et al., 2002, *AJ*, 123, 485  
 Takada M., Hamana T., 2003, *MNRAS*, 346, 949  
 Thomas P. A., Webster R. L., Drinkwater M. J., 1995, *MNRAS*, 273, 1069  
 Tyson J. A., 1986, *AJ*, 92, 691  
 Verde L., et al., 2002, *MNRAS*, 335, 432  
 Webster R. L., Hewett P. C., Harding M. E., Wegner G. A., 1988, *Nature*, 336, 558  
 Williams L. L. R., Frey N., 2003, *ApJ*, 583, 594  
 Williams L. L. R., Irwin M., 1998, *MNRAS*, 298, 378  
 Willmer C. N. A., da Costa L. N., Pellegrini P. S., 1998, *AJ*, 115, 869  
 Wilson G., 2003, *ApJ*, 585, 191  
 Yasuda N., et al., 2001, *AJ*, 122, 1104  
 Zehavi I., et al., 2002, *ApJ*, 571, 172

## APPENDIX A: GAZTAÑAGA MODEL

The model reviewed in this appendix is described in detail by Gaztañaga (2003; see also Myers 2003).

Groth & Peebles (1977) and Phillipps et al. (1978) proposed the ‘ $\epsilon$ ’ form of the (three-dimensional) correlation function to describe the evolution of clustering with redshift

$$\xi(r, z) = \left(\frac{r_0}{r}\right)^\gamma (1+z)^{-(3+\epsilon)} \quad (\text{A1})$$

For the purposes of this model we shall assume that  $\epsilon = 0$ , corresponding to the stable clustering regime, in reasonable agreement with both current observational evidence and theoretical considerations (Wilson 2003; Carlberg et al. 2000; Hamilton et al. 1991; Peacock & Dodds 1994) for the small-scale correlations of lensing matter we consider, at the low redshifts ( $z \sim 0.15$ ) where our galaxy samples reside.

As at the median depth of our galaxy samples ( $z \sim 0.15$ ), 1 arcmin corresponds to  $0.1 h^{-1} \text{Mpc}$ , we choose to measure fluctuations on this scale. The volume-averaged integral of the mass correlation function,  $\xi$ , over a sphere of radius  $R$  is (Peebles 1980)

$$\bar{\xi}(R) = \sigma_{0.1}^2 \left(\frac{0.1 h^{-1} \text{Mpc}}{R}\right)^\gamma \quad (\text{A2})$$

with

$$\sigma_{0.1}^2 = \frac{72}{(3-\gamma)(4-\gamma)(6-\gamma)2^\gamma} \left(\frac{r_0}{0.1 h^{-1} \text{Mpc}}\right)^\gamma. \quad (\text{A3})$$

Gaztañaga (2003) has shown that a good power-law expression for scale-dependent biasing of galaxies is

$$b(R) = b_{0.1} \left(\frac{0.1 h^{-1} \text{Mpc}}{R}\right)^{\gamma_b} \quad (\text{A4})$$

Whilst Gaztañaga assumed that this bias corresponded to the ratio of the galaxy and matter correlation functions;  $b(r) = [\xi_{gg}(r)/\xi_{mm}(r)]^{0.5}$ , we are in fact comparing the cross-correlation of QSOs and galaxies with the galaxy auto-correlation function, and so are defining a bias function via  $b(r) = \xi_{gg}(r)/\xi_{gm}(r)$ . Whilst on large scales these two definitions should be equal, one expects the halo of the central

galaxy to affect the shape of  $\xi_{gm}(r)$  on small scales. Therefore we consider a revised version of the Gaztañaga model to take this into account.

Firstly we define the volume-averaged galaxy-mass cross-correlation,  $\bar{\xi}_{gm}(R)$  via,

$$\bar{\xi}_{gm}(R) = b^* \left( \frac{0.1 h^{-1} \text{Mpc}}{R} \right)^{\gamma^*} \times \bar{\xi}(R). \quad (\text{A5})$$

In the case where the two definitions of bias given above agree exactly,  $b^* = b_{0.1}$  and  $\gamma^* = \gamma_b$ .

The galaxy-averaged correlation function can thus be expressed in terms of the mass-averaged function of Equation A2 as

$$\bar{\xi}_g(R) = b_{0.1} b^* \sigma_{0.1}^2 \left( \frac{0.1 h^{-1} \text{Mpc}}{R} \right)^{\gamma + \gamma^* + \gamma_b}. \quad (\text{A6})$$

The two-dimensional projection of the galaxy correlation function is (again consider Peebles 1980)

$$\omega_{gg}(\theta) = \sigma_{0.1}^2 b_{0.1} b^* \theta^{1-\gamma_{gg}} A_{gg,0.1} \quad (\text{A7})$$

where

$$A_{gg,0.1} = B_{0.1}(\gamma_{gg}) \int d\chi \left( \frac{dN_g}{d\chi} \right)^2 \chi^{1-\gamma_{gg}} (1+z)^{-(3+\epsilon)} \quad (\text{A8})$$

with

$$B_a(\gamma) = \frac{\gamma(3-\gamma)(4-\gamma)(6-\gamma)2^\gamma \Gamma(1/2)\Gamma(\gamma/2-1/2)}{a^{-\gamma} 72 \Gamma(\gamma/2)} \quad (\text{A9})$$

and  $\gamma_{gg} = \gamma + \gamma^* + \gamma_b$ . Note that  $dN_g/d\chi$  is the galaxy radial selection function as a function of comoving distance,  $\chi$ , which is easily derived from the normalised redshift distribution of the galaxies (Gaztañaga 2003). We use the selection function of Baugh and Efstathiou (1993) to model the redshift distribution of our galaxies.

In the weak lensing approximation, we can relate the fluctuations in projected QSO numbers due to lensing to the convergence via (Bartelmann 1995; Bartelmann & Schneider 2001; Menard & Bartelmann 2002)

$$\delta_\mu(\theta) = (2.5\alpha - 1)\delta\mu = 2(2.5\alpha - 1)\kappa_{\text{eff}}(\theta) \quad (\text{A10})$$

$$= \int d\chi \varepsilon(\chi) \delta(\theta, \chi). \quad (\text{A11})$$

where  $\delta(\theta, \chi)$  is the density contrast of the underlying lensing matter. The lensing efficiency,  $\varepsilon(\chi)$ , is defined (Bernardeau, van Waerbeke & Mellier 1997) as

$$\varepsilon(\chi) = (2.5\alpha - 1) \frac{3H_0^2 \Omega_m}{c^2} (1+z) \chi \int_\chi^\infty d\chi' \frac{\chi' - \chi}{\chi'} \frac{dN_q}{d\chi'} \quad (\text{A12})$$

where  $dN_q/d\chi$  is the QSO selection function in comoving coordinates, which we derive from the redshift distribution of (quality ‘11’,  $z > 0.4$ ) QSOs in the 2QZ sample.

As outlined in Gaztañaga (2003), these equations allow us to derive the galaxy-QSO cross-correlation.

$$\omega_{gq}(\theta) = \sigma_{0.1}^2 b^* \theta^{1-\gamma_{gq}} A_{gq,0.1} \quad (\text{A13})$$

where

$$A_{gq,0.1} = B_{0.1}(\gamma_{gq}) \int d\chi \left( \frac{dN_g}{d\chi} \right) \varepsilon(\chi) \chi^{1-\gamma_{gq}} (1+z)^{-(3+\epsilon)} \quad (\text{A14})$$

where  $\gamma_{gq} = \gamma + \gamma^*$ .  $\varepsilon(\chi)$  is typically less than 1 per cent of  $\frac{dN_g}{d\chi}$ , which often leads to the prediction that  $\omega_{gq}$  should

only be observed to be a tiny fraction of  $\omega_{gg}$  (Dolag & Bartelmann 1997).

The slope of the bias correlation function,  $\gamma_b$ , can be easily determined from  $\gamma_{gg}$  and  $\gamma_{gq}$ . The bias parameter,  $b_{0.1}$  can be determined via

$$b_{0.1} = \frac{\omega_{gq}(\theta) A_{gq,0.1} \theta^{\gamma_b}}{\omega_{gg}(\theta) A_{gg,0.1}} \quad (\text{A15})$$

If the two definitions of bias given above agree exactly,  $b^* = b_{0.1}$  and  $\gamma^* = \gamma_b$ , and one could further derive the slope of the mass correlation function,  $\gamma$ , and  $\sigma_{0.1}$  via

$$\sigma_{0.1}^2 = \frac{\omega_{gq}(\theta)^2 A_{gq,0.1} \theta^{\gamma-1}}{\omega_{gg}(\theta) A_{gg,0.1}^2}. \quad (\text{A16})$$